

The Correlation of the Interstellar Extinction Law with the Wavelength of Maximum Polarization

D. C. B. Whittet* and I. G. van Breda**

University Observatory, St. Andrews, Fife, KY16 9LZ, Scotland

Received December 12, 1977

Summary. Infrared photometry is presented for 56 Southern early-type stars which have interstellar polarization data available in the literature. New and previously published data are combined to investigate the relationship between the colour excess ratio E_{V-K}/E_{B-V} and the wavelength of maximum polarization (λ_{\max}). A high degree of linear correlation is found when stars with spectral peculiarities associated with mass loss and circumstellar shells are excluded. The dependence of λ_{\max} on the ratio of total to selective extinction ($R = A_V/E_{B-V}$) is deduced for normal stars to be

$$R = (5.6 \pm 0.3) \lambda_{\max}, \quad (\lambda_{\max} \text{ in } \mu\text{m})$$

which provides substantial confirmation of the result of Serkowski, Mathewson and Ford. The scatter in the λ_{\max} vs. E_{V-K}/E_{B-V} diagram for the peculiar stars probably results from circumstellar infrared emission rather than intrinsic polarization. It is concluded that λ_{\max} is generally a more reliable grain size parameter than R , and that the relation

$$A_V = 5.6 \lambda_{\max} E_{B-V}$$

provides the best means of determining the visual absorption for individual stars. If the normal λ_{\max} -extinction law correlation holds in the Orion nebula, R values no greater than 4.0 are implied.

Key words: infrared photometry — interstellar extinction and polarization — infrared excess

1. Introduction

The polarization of starlight has assumed a particular significance in recent years in the study of interstellar grains. The presence of polarization has long been at-

tributed to the partial alignment of non-spherical grains by the galactic magnetic field, although details of the alignment mechanism still pose theoretical problems (see, e.g., Martin, 1971). Observations of linear and circular polarization give information on both the size and the composition of the grains. Serkowski and co-workers have recently demonstrated that the wavelength of maximum linear polarization, λ_{\max} , is a characteristic grain size parameter. Normalization of measurements relative to λ_{\max} appears to provide a unique relationship for the interstellar polarization curve of the form

$$(P/P_{\max}) = \exp [-k \ln^2 (\lambda_{\max}/\lambda)] \quad (1)$$

(Serkowski, 1973; Coyne et al., 1974). These authors regarded k as a constant in Equation (1), but Codina-Landaberry and Magalhães (1976) have shown that the fit to observational curves can be further improved by allowing k to vary. Comparison of λ_{\max} values with the cross-over wavelength of circular polarization, λ_c , gives a means of evaluating the absorption constant of the grain material (Martin, 1974), and results so far available indicate the grains to be composed purely of dielectrics (Martin and Angel, 1976; McMillan and Tapia, 1977), a conclusion in satisfactory agreement with constraints applied by cosmic abundances. It should be noted that these results apply only to the larger component of the dust responsible for the visual/infrared polarization and extinction, and not to the smaller species invoked to explain the ultraviolet extinction curve and the diffuse bands.

As the value of λ_{\max} is expected to vary with the mean grain radius, a correlation with the ratio of total to selective extinction, $R = A_V/E_{B-V}$, is implied. Serkowski et al. (1975, hereafter referred to as SMF) deduced from a plot of λ_{\max} against the colour excess ratio E_{V-K}/E_{B-V} (their Fig. 8) that

$$R = 5.5 \lambda_{\max} \quad (\lambda_{\max} \text{ in } \mu\text{m}). \quad (2)$$

However, their plot contained considerably more scatter than might be expected from observational errors, and

Send offprint requests to: D. C. B. Whittet

* Present address: Department of Physics and Astronomy, University College, Gower Street, London WC1E 6BT, England

** and Royal Greenwich Observatory, Herstmonceux Castle, Hailsham, Sussex BN27 1RP, England

Table 1. Infrared photometry

| Star | <i>J</i> | <i>H</i> | <i>K</i> | <i>L</i> | <i>n</i> |
|----------------|----------|----------|----------|----------|----------|
| HD 37903 | 7.36 | 7.28 | 7.28 | 7.44 | 2 |
| 38051 | 7.60 | 7.49 | 7.51 | 7.55 | 1 |
| NGC 2024 No. 1 | 7.35 | 6.39 | 5.86 | 5.60 | 1 |
| 46484 | 6.94 | 6.85 | 6.78 | 6.91 | 1 |
| 46485 | 7.52 | 7.40 | 7.38 | 7.43 | 1 |
| 47240 | 5.75 | 5.73 | 5.71 | 5.76 | 1 |
| 47432 | 5.87 | 5.86 | 5.83 | 5.93 | 1 |
| 50064 | 6.21 | 5.86 | 5.64 | 5.51 | 1 |
| 52721 | 6.29 | 6.23 | 6.10 | 5.96 | 2 |
| 62150 | 6.53 | 6.33 | 6.23 | 6.16 | 3 |
| 69882 | 6.42 | 6.34 | 6.30 | 6.29 | 2 |
| 73882 | 6.13 | 5.99 | 5.93 | 5.93 | 4 |
| 78785 | 7.44 | 7.31 | 7.26 | 7.31 | 1 |
| 80077 | 4.41 | 3.93 | 3.63 | 3.38 | 5 |
| 80558 | 4.59 | 4.40 | 4.28 | 4.09 | 2 |
| 90772 | 3.46 | 3.24 | 3.07 | 2.96 | 1 |
| 91619 | 5.10 | 4.90 | 4.79 | 4.42 | 2 |
| 92207 | 4.05 | 3.77 | 3.59 | 3.46 | 2 |
| 93206 | 5.56 | 5.36 | 5.33 | 5.10 | 2 |
| 94909 | 6.21 | 6.06 | 5.97 | 5.94 | 3 |
| 99953 | 5.67 | 5.53 | 5.43 | 5.31 | 2 |
| 100262 | 3.95 | 3.72 | 3.60 | 3.43 | 2 |
| 110432 | 4.50 | 4.28 | 3.96 | 3.50 | 6 |
| 112244 | 5.28 | 5.27 | 5.25 | 5.20 | 4 |
| 113034 | 6.81 | 6.47 | 6.26 | 6.09 | 1 |
| 113422 | 6.37 | 6.11 | 5.95 | 5.79 | 2 |
| 114340 | 6.83 | 6.65 | 6.51 | 6.35 | 2 |
| 120678 | 7.37 | 7.15 | 6.88 | 6.56 | 2 |
| 122879 | 6.07 | 6.03 | 6.00 | 5.99 | 4 |
| 124314 | 6.40 | 6.35 | 6.30 | 6.22 | 1 |
| 125835 | 4.42 | 4.20 | 4.08 | 4.01 | 3 |
| 134959 | 5.82 | 5.48 | 5.29 | 5.09 | 4 |
| 147165 | 2.47 | 2.41 | 2.37 | 2.40 | 1 |
| 147888 | 5.75 | 5.60 | 5.49 | 5.45 | 3 |
| 147889 | 5.39 | 4.89 | 4.56 | 4.38 | 1 |
| 147932 | 6.16 | 5.90 | 5.77 | 5.70 | 3 |
| 148184 | 3.50 | 3.29 | 3.04 | 2.71 | 2 |
| 148937 | 5.88 | 5.80 | 5.69 | 5.54 | 1 |
| 149019 | 5.21 | 4.90 | 4.72 | 4.63 | 2 |
| 149757 | 2.59 | 2.62 | 2.62 | 2.70 | 1 |
| 153919 | 5.76 | 5.65 | 5.54 | 5.46 | 2 |
| 154445 | 5.28 | 5.33 | 5.29 | 5.35 | 2 |
| 157038 | 4.54 | 4.29 | 4.11 | 3.97 | 2 |
| 160529 | 3.68 | 3.22 | 2.93 | 2.65 | 2 |
| 161056 | 5.53 | 5.39 | 5.32 | 5.30 | 2 |
| 161961 | 7.37 | 7.37 | 7.35 | 7.37 | 1 |
| 162978 | 6.03 | 6.02 | 6.00 | 5.98 | 2 |
| 163800 | 6.37 | 6.34 | 6.29 | 6.27 | 2 |
| 164740 | 7.95 | 7.39 | 6.64 | 5.23 | 2 |
| 168607 | 4.41 | 3.82 | 3.39 | 2.99 | 2 |
| 168625 | 5.01 | 4.48 | 4.13 | 3.68 | 2 |
| 170740 | 5.22 | 5.21 | 5.18 | 5.16 | 2 |
| 170836 | 8.21 | 8.16 | 8.12 | 8.12 | 2 |
| 179406 | 5.06 | 5.06 | 5.03 | 5.03 | 2 |
| 184915 | 5.02 | 5.05 | 5.04 | 5.01 | 2 |
| 203532 | 6.11 | 6.12 | 6.05 | 6.05 | 2 |

the reliability and uniqueness of Equation (1) is therefore open to considerable doubt. Martin and Angel (1976) commented that the correlation between λ_{\max} and λ_c is tighter than that between λ_{\max} and *R*. It has been shown by several investigators that λ_{\max} and *R* are increased in

dense dark clouds associated with star formation. Large systematic variations in the general extinction law have been ruled out, but Whittet (1977) has demonstrated that there is evidence for a small but significant variation in both *R* and λ_{\max} with galactic longitude. Thus λ_{\max} measurements could provide a valuable means of studying variations in the extinction law on both a local and a galactic scale. It is therefore very important to establish whether the scatter in the $\lambda_{\max}-E_{V-K}/E_{B-V}$ diagram is intrinsic to the interstellar medium, or whether it is due to observational or intrinsic colour matching errors or to circumstellar effects.

This paper presents the results of a programme of infrared photometry for Southern stars for which λ_{\max} values are available in the literature. The number of stars available for analysis of the λ_{\max} -extinction ratio correlation is thus increased by a factor of more than two, giving a sample large enough to allow distributions for different classes of stars to be compared.

2. Observations

Infrared observations were made at the Sutherland site of the South African Astronomical Observatory during three observing runs on the 1.9 m telescope in 1976 April, 1977 March and 1977 July, using the photometer described by Glass (1973). The 0.75 m telescope was also used during 1976 April to observe a few of the brighter stars. No systematic differences were found between measurements made on the two telescopes. The data were reduced using the FORTH programming system on the Nova 820 minicomputer at St. Andrews, and results were tied to the standard JHKL photometric system using standard stars from the list of Glass (1974). Photometry is presented in the four bands (effective wavelengths 1.25, 1.65, 2.2 and 3.4 μm) in Table 1 for a total of 56 stars selected from the polarization catalogues of SMF and Coyne et al. (1974). Stars noted as having variable polarization were rejected, as were stars with low reddening ($E_{B-V} < 0.25$). The number of separate observations averaged for each star is given in column 6 of the table. The mean error of a single observation is $\pm 0^{\text{m}}03$ at *J*, *H* and *K*, while at *L* the errors are $\pm 0^{\text{m}}05$ for stars brighter than $L=7^{\text{m}}0$, rising to $\pm 0^{\text{m}}08$ at $L=7^{\text{m}}5$ and $\pm 0^{\text{m}}15$ at $L=8^{\text{m}}0$.

3. The $\lambda_{\max}-E_{V-K}/E_{B-V}$ Diagram

K magnitudes from Table 1 were combined with *UBV* photometry and MK spectral types, taken mainly from the catalogues of Blanco et al. (1968) and Kennedy and Buscombe (1974), to deduce values of E_{V-K}/E_{B-V} for each star using intrinsic colours tabulated by Johnson (1966). These results were combined with previously published infrared data (SMF and references therein; van Breda et al., 1974; Whittet et al., 1976; van Breda and Whittet, 1977; McMillan, 1977), bringing the total

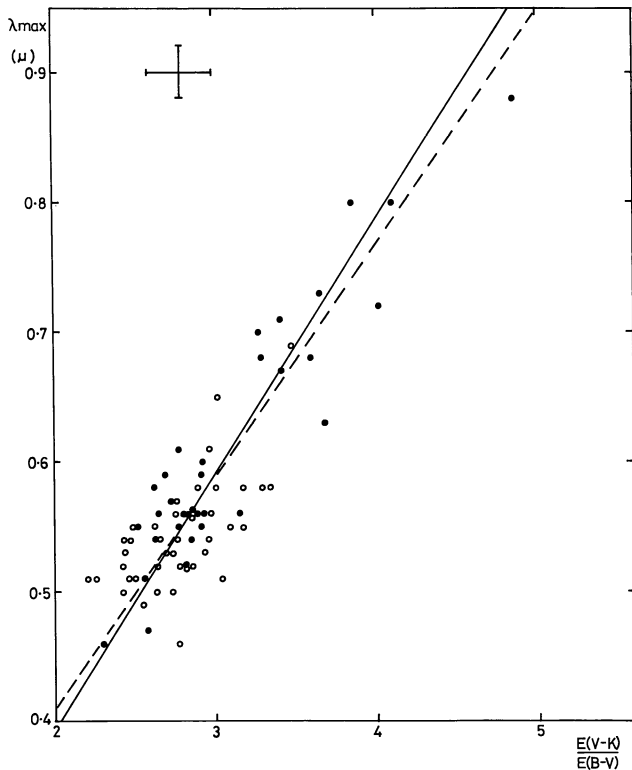


Fig. 1. Plot of λ_{\max} against E_{V-K}/E_{B-V} for normal stars. Open circles represent supergiants and filled circles stars of lower luminosity. The broken line is the best straight line by least squares and the continuous line is that passing through the origin. The cross at top left indicates mean error limits

number of stars for the analysis to 98. Where photometry is available from more than one source a mean is taken.

We must consider the possibility that scatter in the $\lambda_{\max}-E_{V-K}/E_{B-V}$ diagram (SMF, Fig. 8) results from stellar or circumstellar effects in the form of infrared excess radiation or intrinsic polarization. The stars were therefore divided into two groups. Group 1 contains 73 stars with apparently normal spectra, and includes all luminosity classes except Ia^+ . Other supergiants which have emission or P Cygni profiles at the $H\alpha$ line only are regarded as normal: Barlow and Cohen (1977) consider that such stars do not have significant circumstellar infrared emission at wavelengths shorter than $10\ \mu\text{m}$. Group 2 comprises 25 stars with spectral peculiarities associated with circumstellar shells. This includes superluminous supergiants (Class Ia^+) which probably suffer mass loss (see, e.g., Hutchings, 1976), as well as Be, Bp, Oe, Of and On stars. We shall refer to Groups 1 and 2 as the "normal" and the "peculiar" stars respectively.

3.1 The Normal Stars

A plot of λ_{\max} vs. E_{V-K}/E_{B-V} for the normal stars is presented in Figure 1. Open circles represent supergiants

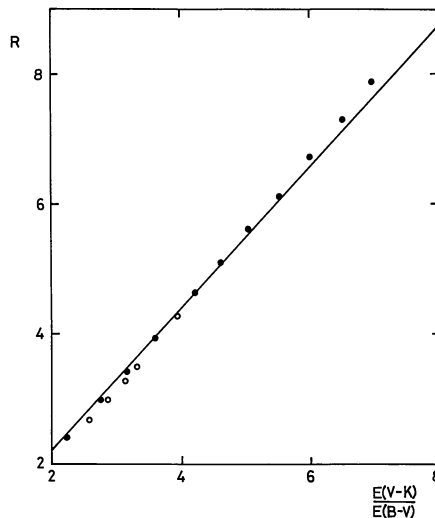


Fig. 2. Plot of R against E_{V-K}/E_{B-V} for an ice grain model (filled circles) and a graphite-iron-silicate grain model (open circles). The straight line represents $R=1.1 E_{V-K}/E_{B-V}$

and filled circles stars of lower luminosity. The cross at top left gives mean observational error limits. Two lines are fitted to the points: the broken line is the best straight line according to least squares, and the continuous line is that constrained to pass through the origin.

Figure 1 enables us to draw several conclusions. The degree of correlation is high (correlation coefficient 0.88). The scatter relative to the best straight line is notably less than that found by SMF, and is generally compatible with observational errors. The 40 supergiants show an obvious clustering towards low λ_{\max} values, only 3 lying outside the range $0.49-0.61\ \mu\text{m}$. This is due to the selection effect noted by SMF: distant, luminous stars are generally seen through diffuse interstellar clouds with normal extinction laws, whereas nearby stars with polarizations high enough to give a measurable λ_{\max} value usually lie in dense clouds where larger values can be expected. The supergiants nevertheless appear to follow the same general correlation as the lower luminosity stars. The fact that Figure 1 includes stars from NGC 2264, the Ophiuchus dark cloud and the Orion association, as well as supergiants distributed around the Milky Way suggests the existence of a unique relationship. The best straight line has the equation

$$E_K = a \lambda_{\max} + b,$$

where

$$E_K = E_{V-K}/E_{B-V}$$

and the constants a and b have values

$$a = 5.6 \pm 0.7,$$

$$b = -0.3 \pm 0.4.$$

The best straight line through the origin is

$$E_K = m \lambda_{\max},$$

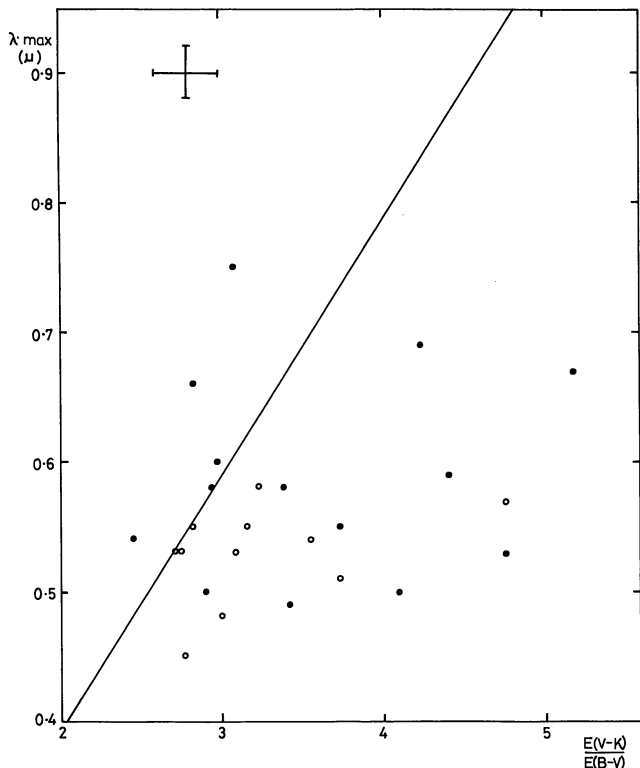


Fig. 3. Plot of λ_{\max} against E_{V-K}/E_{B-V} for peculiar stars. Open circles represent supergiants as in Figure 1. The straight line represents $\lambda_{\max} = 5.1 E_{V-K}/E_{B-V}$. The cross at top left indicates mean error limits

where

$$m = \langle E_K \rangle / \langle \lambda_{\max} \rangle = 5.08.$$

There are no theoretical reasons for supposing that the relationship between λ_{\max} and E_K should or should not pass through the origin. The results given here do not present strong support for the inclusion of an additive constant, and we follow SMF in adopting a straightforward proportionality:

$$E_K = (5.1 \pm 0.3) \lambda_{\max}. \quad (3)$$

The relationship between E_K and the ratio of total to selective extinction is usually taken as

$$R = 1.1 E_K, \quad (4)$$

which is precise for the normal van de Hulst theoretical curve No. 15 with $R = 3.05$. To check the general applicability of Equation (4) to other values of R , theoretical curves were computed from the Mie theory for a range of grain sizes. Figure 2 shows a plot of R vs. E_K for dielectric grains of constant refractive index $n = 1.3$ (filled circles) and for the composite grain model assumed by Whittet et al. (1976, open circles). The straight line represents Equation (4). There is a tendency for the filled circles to rise above the line for high R values, and for the open circles to lie slightly below the line. However, Equation (4) may be assumed for $E_K < 6$ without risk of

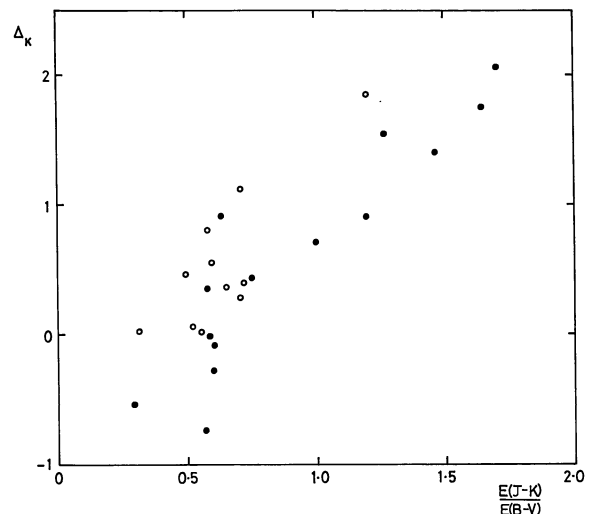


Fig. 4. Plot of Δ_K against E_{J-K}/E_{B-V} for stars in Table 2. Open circles represent supergiants

introducing errors of more than 5% in resulting R values. Combining Equations (3) and (4), R and λ_{\max} are related by

$$R = (5.6 \pm 0.3) \lambda_{\max}. \quad (5)$$

3.2 The Peculiar Stars

Figure 3 shows the $\lambda_{\max} - E_{V-K}/E_{B-V}$ diagram for the 25 peculiar stars, with the line deduced for normal stars [Eq. (3)] superposed. Again the supergiants are represented by open circles. The contrast between Figures 3 and 1 is striking. It should be noted that the mean errors are no larger in Figure 3, and there is thus a genuine departure from the normal star distribution with points tending to lie to the right of the line. Only two stars lie significantly to the left, and one of these (HD 163 800) has considerable uncertainty in its λ_{\max} value (SMF, Table 5).

If the difference is caused by circumstellar effects, it could result from either infrared emission shifting points from left to right in the diagram, or intrinsic polarization producing a trend towards lower λ_{\max} values, or a combination of both. If the scatter is caused by infrared emission, a correlation is expected between the deviation from the best straight line for normal stars, given by

$$\Delta_K = E_K - 5.1 \lambda_{\max} \quad (6)$$

and the colour excess ratio E_{J-K}/E_{B-V} , which should be sensitive to dips in the extinction curve caused by emission at K . Data for the peculiar stars are listed in Table 2. Figure 4 shows a plot of Δ_K against E_{J-K}/E_{B-V} . A strong correlation is apparent, which indicates that the stars with high Δ_K must have either infrared excesses or peculiar extinction curves with high R values. Figure 5 shows a plot of R value [deduced from Eq. (5)] against E_{J-K}/E_{B-V} for the normal stars, with the relationship expected from theoretical curves (continuous line) su-

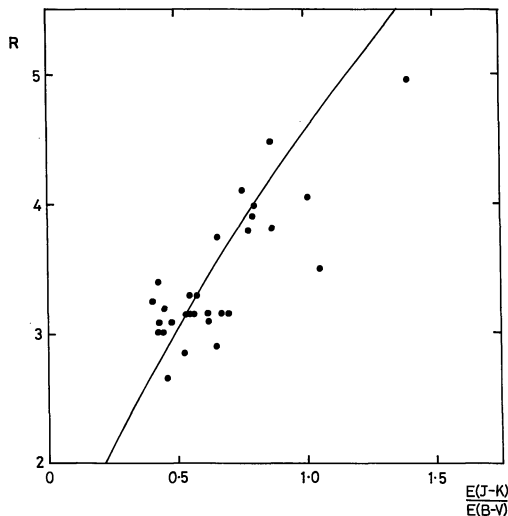


Fig. 5. Plot of R against E_{J-K}/E_{B-V} for normal stars. The curve represents the expected theoretical relation

perposed. We see from Figure 5 that $E_{J-K}/E_{B-V} \approx 0.5$ for R values close to 3, and that R values in excess of 5 would be required to explain the stars with highest E_{J-K}/E_{B-V} in Figure 4. These stars could have extinction components which produce genuinely high R values but do not contribute sufficiently to the polarization to produce a corresponding increase in λ_{\max} . Such an effect could be induced by circumstellar shells of large non-aligned or spherical grains. An abnormally low value of the ratio of polarization to reddening would be expected for such stars. Values of P_{\max}/E_{B-V} are plotted against Δ_K for the peculiar stars in Figure 6. The expected decrease in P_{\max}/E_{B-V} for high Δ_K is not apparent (indeed, the reverse appears more likely to be true), which argues against this interpretation.

The polarization curves of unreddened Be stars are characterised by a peak in the blue ($\lambda \approx 0.45 \mu\text{m}$) and a sharp drop towards the ultraviolet (Kruszewski et al., 1969). The degree of polarization is small, however, and Be stars with appreciable reddening exhibit a wavelength-dependence which is predominantly interstellar. The case for significant intrinsic polarization is further weakened by a comparison of λ_{\max} values for stars with high Δ_K with those for other stars in the same regions of sky. For example, HD 164740 has essentially the same λ_{\max} value ($0.67 \mu\text{m}$) as the two stars closest to it in the sky in the SMF catalogue. Similarly, HD 110432 in the Coal Sack has a λ_{\max} value ($0.59 \mu\text{m}$) entirely compatible with those of other stars in this region of the Milky Way (see, e. g., Whittet, 1977). We therefore deduce that intrinsic polarization is not an important factor in determining the positions of the peculiar stars in the $\lambda_{\max} - E_{V-K}/E_{B-V}$ diagram, and that the scatter in Figure 3 is very probably the result of circumstellar infrared emission affecting approximately half the stars plotted.

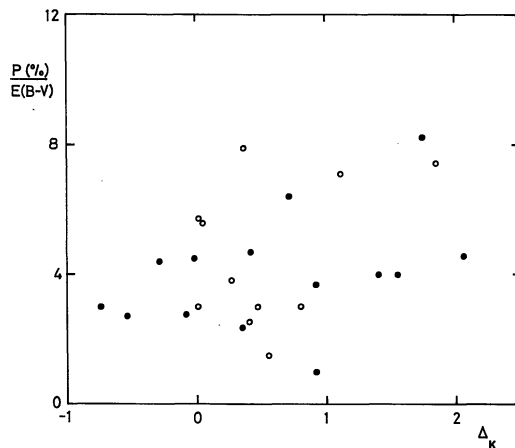


Fig. 6. Plot of P_{\max}/E_{B-V} against Δ_K for stars in Table 2. Open circles represent supergiants

In a recent paper Breger (1977) has examined the $\lambda_{\max} - E_{V-K}/E_{B-V}$ diagram for stars in the Orion nebula. He found a distribution rather similar to our Figure 3, with a trend towards the right of the diagram relative to the normal relation. As several of the stars he plotted are suspected shell stars, infrared excesses are again a likely cause of the scatter, although Breger argues that the normal λ_{\max} -extinction ratio correlation does not hold in the Orion nebula.

4. Conclusions

We have deduced that the ratio of total to selective extinction and the wavelength of maximum polarization are related by the formula

$$R = 5.6 \lambda_{\max},$$

thus providing strong confirmation of the results of SMF. In particular, our results indicate that there is no evidence for intrinsic scatter in the $\lambda_{\max} - E_{V-K}/E_{B-V}$ diagram (Fig. 1): the scatter remaining when classes of stars likely to have infrared excesses are excluded is compatible with observational errors. We therefore conclude that λ_{\max} is, in general, a more reliable grain size parameter than R , and the relation

$$A_V = 5.6 \lambda_{\max} E_{B-V}$$

is thus currently the most reliable method of determining the visual absorption for individual stars. This result provides further support for the conclusion of Whittet (1977) that systematic variations in mean λ_{\max} values for different galactic regions imply a small but significant variation in the general extinction law with galactic longitude. The range of this variation is $0.52 - 0.58 \mu\text{m}$ in λ_{\max} , equivalent to $2.93 - 3.25$ in R . The overall mean

Table 2. Data for the peculiar stars

| Star | <i>Sp</i> | λ_{\max} (μm) | $\frac{E_{V-K}}{E_{B-V}}$ | $\frac{E_{J-K}}{E_{B-V}}$ | Δ_K | Remarks |
|----------------|------------------------|------------------------------------|---------------------------|---------------------------|------------|--------------|
| HD 15570 | O4If | 0.53 | 2.71 | 0.31 | 0.01 | |
| 24912 | O7.5IIIInf | 0.58 | 2.94 | 0.58 | -0.02 | |
| NGC 2024 No. 1 | B0.5Vp | 0.69 | 4.23 | 1.00 | 0.71 | ^a |
| 52721 | B2Vne | 0.50 | 4.10 | 1.27 | 1.55 | |
| 73882 | O8n | 0.75 | 3.08 | 0.57 | -0.74 | |
| 80077 | B2Ia ⁺ e | 0.55 | 2.82 | 0.55 | 0.01 | ^b |
| 92207 | A0Iae | 0.51 | 3.71 | 0.71 | 1.11 | |
| 93206 | O9.7Ibn | 0.57 | 4.76 | 1.19 | 1.85 | |
| 110432 | B2pe | 0.59 | 4.41 | 1.46 | 1.40 | |
| 114340 | B1Ia ⁺ | 0.55 | 3.16 | 0.65 | 0.36 | |
| 120678 | Ope | 0.53 | 4.76 | 1.71 | 2.06 | |
| 124314 | O8nk | 0.54 | 2.46 | 0.60 | -0.29 | |
| 148184 | B2IVe | 0.55 | 3.71 | 1.19 | 0.91 | |
| 148688 | B1Ia ⁺ e | 0.53 | 3.09 | 0.72 | 0.39 | |
| 148937 | O6Vf | 0.60 | 2.97 | 0.61 | -0.09 | |
| 152236 | B1.5Ia ⁺ pe | 0.58 | 3.23 | 0.71 | 0.27 | ^c |
| 153919 | O6f | 0.58 | 3.38 | 0.74 | 0.42 | ^d |
| 157038 | B4Ia ⁺ | 0.54 | 3.55 | 0.58 | 0.80 | |
| 160529 | A2Ia ⁺ | 0.53 | 2.75 | 0.52 | 0.05 | |
| 163800 | O7IIIf | 0.66 | 2.83 | 0.29 | -0.54 | |
| 164740 | O7(e) | 0.67 | 5.17 | 1.64 | 1.75 | ^e |
| 166734 | O8f | 0.50 | 2.91 | 0.58 | 0.36 | |
| 168607 | B9Iap | 0.48 | 3.00 | 0.60 | 0.55 | |
| VI Cyg No. 12 | B8Ia ⁺ | 0.45 | 2.77 | 0.50 | 0.47 | |
| 215835 | O6nn | 0.49 | 3.42 | 0.63 | 0.92 | ^f |

^a NGC 2024 No. 1: has an infrared excess attributed to a circumstellar shell (Grasdalen, 1974)

^b HD 80077: superluminous; situated in dust-embedded cluster Pismis 11 (Moffat and FitzGerald, 1977)

^c HD 152236 (ζ_1 Sco): superluminous spectrum variable associated with mass loss (Jaschek and Jaschek, 1973)

^d HD 153919: spectroscopic binary associated with 2 U 1700-37; λ_{\max} value from Avery et al. (1975)

^e HD 164740 (Herschel 36): in M 8; for discussion of spectrum see Woolf (1961)

^f HD 215835: spectroscopic binary in NGC 7380

value of λ_{\max} is 0.545 μm (SMF), equivalent to $R=3.05$: this is in excellent agreement with other determinations of the mean value of R for diffuse interstellar material (see Whittet, 1977 and references therein).

Measures of λ_{\max} in the cold dark clouds associated with ρ Ophiuchi, NGC 2264 and M 78 imply R values in the range 4–6, confirming that grain growth occurs in these dense regions. The largest λ_{\max} value measured in the Orion nebula cluster is 0.71 μm (Breger, 1977) for the apparently normal star BR 545. If the usual correlation holds a maximum R value of 4.0 is indicated, which is consistent with the conclusion reached by Penston et al. (1975) that the mean extinction law in the Orion nebula does not differ greatly from normal extinction. However, Breger deduced $R \approx 5.6$ for BR 545 from infrared photometry and from luminosity/cluster distance considerations. A breakdown in the normal $R - \lambda_{\max}$ correlation, possibly due to local changes in grain composition, cannot be ruled out in this case.

The scatter in the $\lambda_{\max} - E_{V-K}/E_{B-V}$ diagram for the peculiar stars (Fig. 3) is very probably due to infrared excess radiation affecting the K magnitudes, as indicated by the correlation between Δ_K and E_{J-K}/E_{B-V} (Fig. 4).

Intrinsic polarization does not appear to significantly affect the λ_{\max} values of appreciably reddened emission line stars. Evaluation of Δ_K [Eq. (6)] provides a means of measuring the infrared emission: the excess radiation in magnitudes at $\lambda=2.2 \mu\text{m}$ is $\Delta_K E_{B-V}$. The stars with largest excesses in Table 2 fall into three groups: supergiants (HD 92207, 93206, 157038), classical Oe/Be stars (HD 52721, 110432, 120678, 148184) and stars associated with nebulosity in regions of recent star formation (NGC 2024 No. 1, HD 164740, HD 215835). Free-free emission in the stellar envelope is a likely cause of the effect (Woolf et al., 1970; Dyck and Milkey, 1972), with radiation from heated circumstellar dust shells also a possibility in the third case. It should be noted that not all superluminous stars have infrared excesses: HD 80077 (B 2 Ia⁺e) and HD 160529 (A 2 Ia⁺) occupy perfectly normal positions in the $\lambda_{\max} - E_{V-K}/E_{B-V}$ diagram.

Acknowledgements. We are indebted to the Panel for the Allocation of Telescope Time for observing time at SAAO and to the Science Research Council for financial support. We are also grateful to the SRC for providing the FORTH facility at St. Andrews.

References

- Avery, R. W., Stokes, R. A., Michalsky, J. J., Ekstrom, P. A.: 1975, *Astron. J.* **80**, 1026
- Barlow, M. J., Cohen, M.: 1977, *Astrophys. J.* **213**, 737
- Blanco, V. M., Demers, S., Douglass, G. G., FitzGerald, M. P.: 1968, *Publ. US Naval Obs.* **21**
- Breger, M.: 1977, *Astrophys. J.* **215**, 119
- Codina-Landaberry, S., Magalhães, A. M.: 1976, *Astron. Astrophys.* **49**, 407
- Coyne, G. V., Gehrels, T., Serkowski, K.: 1974, *Astron. J.* **79**, 581
- Dyck, H. M., Milkey, R. W.: 1972, *Publ. Astron. Soc. Pacific* **84**, 597
- Glass, I. S.: 1973, *Monthly Notices Roy. Astron. Soc.* **164**, 155
- Glass, I. S.: 1974, *Monthly Notes Astron. Soc. South Africa* **33**, 53
- Grasdalen, G. L.: 1974, *Astrophys. J.* **193**, 373
- Hutchings, J. B.: 1976, *Astrophys. J.* **203**, 438
- Jaschek, M., Jaschek, C.: 1973, *Publ. Astron. Soc. Pacific* **85**, 127
- Johnson, H. L.: 1966, *Ann. Rev. Astron. Astrophys.* **4**, 193
- Kennedy, P. M., Buscombe, W.: 1974, MK spectral classifications published since Jaschek's La Plata Catalogue, Evanston
- Kruszewski, A., Coyne, G. V., Gehrels, T.: 1969, Mass Loss from Stars, ed. M. Hack, p. 42
- Martin, P. G.: 1971, *Monthly Notices Roy. Astron. Soc.* **153**, 279
- Martin, P. G.: 1974, *Astrophys. J.* **187**, 461
- Martin, P. G., Angel, J. P. R.: 1976, *Astrophys. J.* **207**, 126
- McMillan, R. S.: 1977, *Astrophys. J.* **216**, L41
- McMillan, R. S., Tapia, S.: 1977, *Astrophys. J.* **212**, 714
- Moffat, A. F. J., FitzGerald, M. P.: 1977, *Astron. Astrophys.* **54**, 263
- Penston, M. V., Hunter, J. K., O'Neill, A.: 1975, *Monthly Notices Roy. Astron. Soc.* **171**, 219
- Serkowski, K.: 1973, *IAU Symposium* **52**, 145
- Serkowski, K., Mathewson, D. S., Ford, V. L. (SMF): 1975, *Astrophys. J.* **196**, 261
- van Breda, I. G., Glass, I. S., Whittet, D. C. B.: 1974, *Monthly Notices Roy. Astron. Soc.* **168**, 551
- van Breda, I. G., Whittet, D. C. B.: 1977, *Astrophys. Space Sci.* **48**, 297
- Whittet, D. C. B.: 1977, *Monthly Notices Roy. Astron. Soc.* **180**, 29
- Whittet, D. C. B., van Breda, I. G., Glass, I. S.: 1976, *Monthly Notices Roy. Astron. Soc.* **177**, 625
- Woolf, N. J.: 1961, *Publ. Astron. Soc. Pacific* **73**, 206
- Woolf, N. J., Stein, W. A., Strittmatter, P. A.: 1970, *Astron. Astrophys.* **9**, 252